Automated detection of coronary artery disease using different durations of ECG segments with convolutional neural network

U. Rajendra Acharya [a,b,c,*], Hamido Fujita [d], Oh Shu Lih [a], Muhammad Adam [a], Jen Hong Tan [a], Chua Kuang Chua [a]

[a] Department of Electronics and Computer Engineering, Ngee Ann Polytechnic, Singapore
[b] Department of Biomedical Engineering, School of Science and Technology, SUSS University, Singapore
[c] Department of Biomedical Engineering, Faculty of Engineering, University of Malaya, Malaysia
[d] Iwate Prefectural University (IPU), Faculty of Software and Information Science, Iwate 020-0693, Japan

ARTICLE INFO

ABSTRACT

Coronary artery disease (CAD) is caused due by the blockage of inner walls of coronary arteries by plaque. This constriction reduces the blood flow to the heart muscles resulting in myocardial infarction (MI). The electrocardiogram (ECG) is commonly used to screen the cardiac health. The ECG signals are nonstationary and nonlinear in nature whereby the transient disease indicators may appear randomly on the time scale. Therefore, the procedure to diagnose the abnormal beat is arduous, time consuming and prone to human errors. The automated diagnosis system overcomes these problems. In this study, convolutional neural network (CNN) structures comprising of *four* convolutional layers, *four* max pooling layers and *three* fully connected layers are proposed for the diagnosis of CAD using *two* and *five* seconds durations of ECG signal segments. Deep CNN is able to differentiate between normal and abnormal ECG with an accuracy of 94.95%, sensitivity of 93.72%, and specificity of 95.18% for Net 1 (two seconds) and accuracy of 95.11%, sensitivity of 91.13% and specificity of 95.88% for Net 2 (5 s). The proposed system can help the clinicians in their accurate and reliable decision making of CAD using ECG signals.

© 2017 Elsevier B.V. All rights reserved.

1. Introduction

Cardiovascular disease (CVD) is one of the main non-communicable diseases (NCDs) worldwide. The NCDs have resulted in more deaths as compared to other diseases combined [46]. Out of the 56 million deaths reported globally in 2012, 38 million are due to NCDs. In fact, nearly half (approximated 17.5 million) of the NCDs death is due to CVDs. Among this, almost 7.4 million deaths are due to coronary artery disease (CAD) [37]. The CVD deaths with aging are predicted to increase to 22.2 million in 2030 [36]. Also, the CVDs are accountable for the increase in healthcare spending and serious lifetime disability [42]. In 2010, CVDs have resulted in US$863 billion spending for direct healthcare and worldwide productivity losses. This figure is projected to reach to US$20 trillion by 2030 [12].

In general, the inflammation of the arterial wall due to multi factorial injuries will result in coronary arteriosclerosis (or plaques build up), which is the primary cause of CAD. As the disease progresses, atherosclerotic deposit starts to develop in the lumen of the coronary arteries. Consequently, these depositions cause the inner surface of coronary arteries and the lumen to become irregular and narrow. Hence, it reduces the perfusion of the blood to the myocardium [14,15,45]. Over time, the atherosclerotic deposits may rupture and subsequently coagulate the blood, which can lead to fatal heart attack. In 2013, it is reported that 370,213 Americans die due to CAD, which is about 1 in every 7 people in the United States [6]. In contrast, an estimated 74,000 people died in 2013 due to CAD in the United Kingdom, which is almost half (45%) of the CVDs deaths [43,44].

Typically, arteriosclerosis is developed in the vessel walls of the coronary arteries. The individual coronary artery is essential for delivering the oxygen-rich blood to the myocardium [11]. For a normal artery, the vessel wall is comprised of *three* layers, namely intima, media and adventitia. The intima is the inner layer which is made up of endothelial cells. The media is the middle layer comprised of smooth muscle cells. Lastly, the adventitia is the outer layer composed of mostly collagen fibers. The arteriosclerosis begins with circulating inflammatory white blood cells (WBCs), cholesterol and hemodynamic forces. Then, the leukocytes and low density lipoprotein (LDL) cholesterol will attach and penetrate to

* Corresponding author
 E-mail addresses: aru@np.edu.sg (U.R. Acharya), HFujita-799@acm.org (H. Fujita).

Normal artery

Endothelial dysfunction

Fatty streak formation

Stable (fibrous) plaque formation
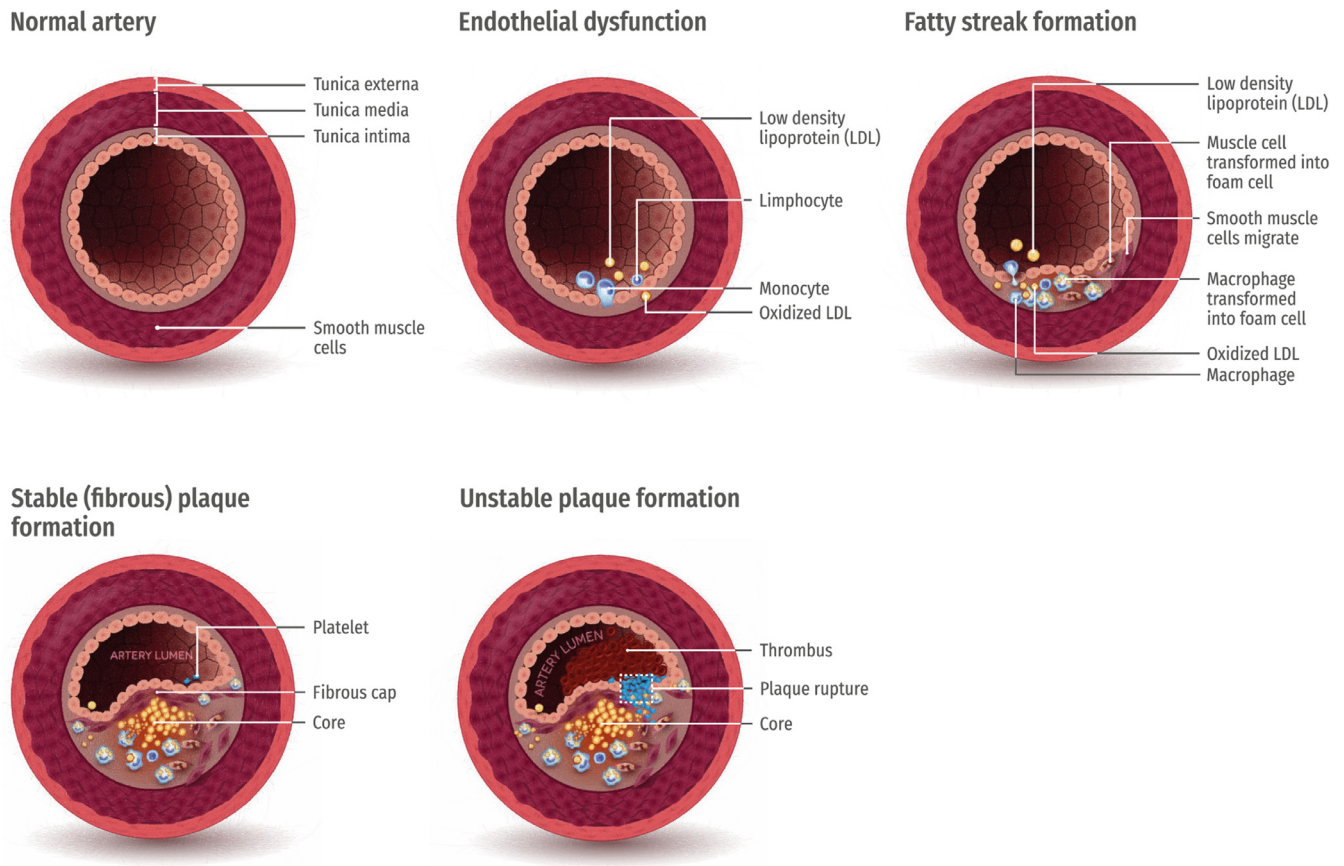
Unstable plaque formation

Fig. 1. The pathology of coronary artery disease (CAD).

the region of the vascular wall where the viscosity and turbulent flow is high. Concurrently, the oxidized LDL cholesterol releases and transforms the macrophages into foam cells, which mainly promotes the formation of fatty deposits. In addition, the oxidized LDL cholesterol encourage the monocytes and smooth muscle cells to migrate to the intima layer where the smooth muscle cells differentiate to produce fibrous encapsulation of the arteriosclerotic plaque. The arteriosclerotic plaque is mainly comprised of the dead and smooth muscle cells. The fibrous encapsulate region of the intima layer progressively grow thicker as smooth muscle cells continue to deposit collagen fibers. Consequently, narrowing the artery lumen which restricts the blood perfusion to the heart muscles. Overall, CAD represents the culmination of the injured vascular wall, triggered inflammatory response, accumulating cholesterol and captured cells as illustrated in Fig. 1 [11]. The degree of stability of atherosclerotic plaque and its clinical manifestation depends on the cellular composition. For a stable plaque, the fibrous encapsulation layer is thick and the presence of smooth muscle cells are in abundance at its core. Conversely, an unstable plaque has a thinner fibrous encapsulation layer and comprised of mostly fat-rich macrophages at its core. Also, this soft and unstable plaque can easily get ruptured and may cause blood clotting. Thus, blocking the blood perfusion may lead to myocardial infarction (or heart attack) [11].

Hence, an early clinical diagnosis is needed to better assist the CAD patients. The clinical vital information on the functioning of the heart is reflected in the ECG signals. The minute changes in the morphology of the ECG beat indicates a cardiac abnormality. Long QT interval and abnormally high T waves imply acute myocardial infarction (MI), but depressed and elevated ST segments indicate sub endocardial and extensive myocardial ischemia respec-

tively [7]. Nevertheless, manually examining the voluminous ECG signals for disease-related morphological changes are tedious and may lead to errors in reading the ECG signals. Also, these disease indicators may appear irregularly in the ECG timescale. Hence, computer aided diagnosis system can be an effective and reliable tool to overcome these inadequacies of manual examination of diseases using ECG signals.

Over the last decade, several algorithms for automated characterization of CAD have been widely developed. These algorithms are implemented using various advanced signal processing methods, such as linear [27,31,32] and nonlinear [5,8,9,16,27,31,32], wavelet transform [20,26,30,38,47] algorithms coupled with artificial intelligence techniques [34,35]. Acharya et al. [1] proposed an automated detection system for CAD and MI using *three* decomposition techniques, namely discrete cosine transform (DCT), empirical mode decomposition (EMD) and discrete wavelet transform (DWT). The proposed system achieved maximum classification accuracy of 98.5%, sensitivity of 99.7% and specificity of 98.5% using only *seven* features extracted from DCT coefficients. The summary of studies conducted on the automated characterization of CAD using ECG and HRV signals is shown in Table 1. These studies are mainly focused on feature extraction and classification processes. The performance of the classifier greatly depends on the distinctive characteristics of the extracted features. Hence, features extraction process is most crucial in characterizing the ECG signals. Furthermore, feature extraction process, normalization, denoising, segmentation, dimension reduction, features selection, and involve a series of *trial and error* manipulation prior to acquiring distinctively significant features for optimal classification results. This process is time consuming and labor intensive as it involves finding and selection of important features. In addition, the computational com-

Table 1
Summary of studies conducted on the automated characterization of CAD using ECG and HRV signals.

HRV signals		
Reference (Year)	Methodology	Performance
Lee et al [32], 2007	Linear features: •Frequency domain •Time domain Nonlinear features: •Poincare plot •Approximate entropy Classifiers: •Support vector machine (SVM) •Classification based on multiple association rules (CMAR) •Naïve Bayesian (NB) •C4.5 (Decision tress)	Acc = 90%
Kim et al [27], 2007	Linear features: •Frequency domain •Time domain Nonlinear features: •Poincare plots •Fractal scaling measures •Complexity estimations Classifiers: • Multiple discriminant analysis (MDA)	Acc = 72.5 ∼ 84.6%
Lee et al [31], 2008	Linear Features: •Frequency domain •Time domain Nonlinear features: •Poincare plot •Hurst exponent •Detrended fluctuation analysis •Approximate entropy Classifiers: •Support vector machine (SVM) •Classification based on multiple association rules (CMAR) •Classification based on predictive association rules (CPAR) •C4.5 (Decision tress) •Multiple discriminant analysis (MDA) •Naïve Bayesian (NB)	Acc = 85 ∼ 90%
Giri et al [20], 2013	Wavelet transform: •Discrete wavelet transform (DWT) Dimensionality reduction techniques: •Principle component analysis (PCA) •Independent component analysis (ICA) •Linear discriminant analysis (LDA) Classifiers: •Support vector machine (SVM) •Gaussian mixture model (GMM) •K-Nearest Neighbors (KNN) •Probabilistic neural network (PNN)	Acc = 96.8% Sen = 100% Spec = 93.7%
Patidar et al [38], 2015	Features: •Tunable Q wavelet transform (TQWT) based decomposition •Correntropy based nonlinear features computed from sub-band of TQWT based decompositions Classifier: •Least squares support vector machine (LS-SVM)	Acc = 99.7% Sen = 99.6% Spec = 99.8%
Sood et al [41], 2016	Features: •Empirical mode decomposition (EMD) •Second-order difference plot area •Analytical signal representation area •Amplitude-modulation bandwidth •Frequency modulation bandwidth •Fourier-Bessel expansion-based mean frequency Classifier •Statistical analysis using *p*-value and Krusal-Wallis	AM and FM bandwidth and FBE-based features are reported to be better at picking up subtle details as compared to ASR and SODP area features
ECG signals		
Reference (Year)	Methodology	Performance
Schreck et al [39], 1988	Features: •Biopotential coordinate transformation (BCT) Classification: •Blinded test •Fisher's exact test	Men: Sen = 84.3% Spec = 81.8% Women: Sen = 76.2% Spec = 80%

Table 1 (*continued*)

HRV signals		
Reference (Year)	Methodology	Performance
Lehtinen et al [34], 1998	Features: ●Artificial neural network Classification: ●Receiver operating characteristics (ROC) analysis	ROC = 91.5%
Lewenstein et al [35], 2001	Features: ●Radial basis function (RBF) neural networks	Average Spec and Sen ≈ 97%
Arafat et al [8], 2005	Features: ●Fuzzy uncertainty classification percentage (CCP) ●Probabilistic uncertainty ●Combined uncertainty	80% correct
Babaoglu et al [9], 2010	Features: ●Principle component analysis (PCA) Classifier: ●Support vector machine (SVM)	Acc = 79.2%
Babaoglu et al [10], 2010	Features selection: ●Binary particle swarm ●Genetic algorithm Classifier: ●Support vector machine	Acc = 81.7%
Yin et al [47], 2011	Features: ●Denoise ●Wavelet decomposition ●R-wave peaks detection ●ST segment detection	Acc = 80%
Kaveh et al [26], 2013	Features: ●Discrete wavelet transform (DWT) ●Principle component analysis (PCA) Classifier: ●Support vector machine (SVM)	Acc = 88%
Acharya et al [5], 2017	Features: ●Bispectrum ●Cumulant Classifiers: ●K-Nearest neighbors (KNN) ●Decision tree (DT)	Bispectrum-KNN: Acc = 98.2% Sen = 94.8% Spec = 99.3%
Kumar et al [30], 2017	Features: ●Flexible analytic wavelet transform(FAWT) ●Cross information potential (CIP) Classifiers: ●Least squares support vector machine (LS-SVM) 2 s and 5 s of ECG segments	Acc = 99.6%
In this study	Methodology Convolutional neural networks (CNNs) (11 layers): ●Four convolutional layers ●Four max pooling layers ●Three fully connected layers	Performance Net A: Acc = 95% Sen = 93.7% Spec = 95.2% Net B: Acc = 95.1% Sen = 91.1% Spec = 95.9%

*Acc = accuracy, PPV = positive predictive value, Sen = sensitivity, Spec = specificity.

plexity of the whole process may significantly increase with huge diverse ECG signals which may alleviate its application as a heart screening toolkit.

There are several signal processing techniques that can be used to extract distinctive information from the ECG signals [4]. Still, the real challenge lies in carefully choosing the appropriate technique and testing the developed model. The signal processing techniques are generally categorized as linear and nonlinear. The linear group is further divided into time and frequency domain measures [19]. The nonlinear techniques used are based on the theory of chaos [18]. The time domain measures are vulnerable to outliers and artifacts, which has an impact on the specificity and sensitivity [3]. In addition, time domain measures may not be particularly reliable in differentiating distinct ECG signals with similar *means* and standard deviations. The frequency domain measures assume that signal is periodic and stationary. However, this assumption is invalid for ECG signals. In order to overcome these problems, nonlinear methods can be used [3].

The automated characterization of heart abnormalities using ECG signal is a challenging task. The system classification performance may significantly vary among patients due to artifacts and even unbalanced classes of ECG signals. Furthermore, notable variations can be observed in morphological and time domain characteristics of ECG signals for different patients during various physical and temporal conditions [24]. Nevertheless, these methodologies performed well only while using training data also for testing (ten-fold cross validation), but not in clinical practice (see Table 1). In real life, ECG signals are different for various

Table 2
Total number of segmented ECG signals used (2 and 5 s).

Type	Number of 2 s segments (Net 1)	Number of 5 s segments (Net 2)
Normal	15,300	6120
CAD	80,000	32,000
Total	**95,300**	**38,120**

classes and factors like age, sex, condition of like diabetes, blood pressure, mental states and life style affecting the signal [15,33].

Therefore, to overcome the limitations present in the methods presented in Table 1, this study proposes the deep learning-based approach for the diagnosis of CAD using ECG signals. In this work, we have used *eleven* layered CNN comprising of convolution layers, subsampling layers and fully connected layers, which are like multilayer perceptron (MLP). The CNNs have performed remarkably well for image analysis and classification [25,29]. Hence, they are likely to detect hidden signatures from the physiological signals without any preprocessing, feature extraction and selection steps.

2. Methodology

2.1. Material used

The normal and CAD ECG signals were retrieved from the Physionet databases, namely Fantasia (for Normal) and St.-Petersburg Institute of Cardiology Technics 12-lead arrhythmia (for CAD) [22]. In this work, we have taken the ECG signals (lead II) from 40 normal (20 males and 20 females) and 7 CAD (1 male and 6 females) subjects. The overview of the number of segmented ECG signals (2 and 5 s) used is shown in Table 2. In this study, a total of 95,300 and 38,120 segmented ECG signals were used for Net 1 (2 s) and Net 2 (5 s) respectively.

2.2. Pre-processing

The ECG signals from the Fantasia database (for Normal) and St.-Petersburg Institute of Cardiology Technics 12-lead arrhythmia database (for CAD) were sampled at 250 Hz and 257 Hz respectively. The ECG signals from Fantasia database (for Normal) were up-sampled to 257 Hz to establish uniformity and standardization of both databases. Subsequently, discrete wavelet transform (DWT) was applied on the ECG signals using Daubechies 6 (db6) mother wavelet to remove the noise and baseline wander [40].

2.3. ECG signal segmentation

Next, the pre-processed normal and CAD ECG signals are segmented into two separate groups Net 1 and Net 2 for *two* and *five* seconds time intervals respectively without any detection of R peaks of the ECG waves. The *five* and *two* second ECG segment consists of 1285 and 514 samples respectively. In addition, Z score normalization technique is implemented to normalize the individual ECG segments. This is to overcome the problem of amplitude scaling and to remove the offset effect prior to feeding the segmented ECG signals to the 1 dimensional (1D) CNN for training and testing. The typical plot of the *two* and *five* second ECG signals are shown in Figs. 2 and 3 respectively.

2.4. Convolutional neural networks (CNNs)

The convolutional neural networks (CNNs) technique is made up of *two* components. The first component is the feature identifier where the features from the input data are automatically learned. The second component is a fully connected multi-layer perceptron (MLP) which carry out classification based on the initially learned

features [48]. Further, the feature identifier component comprises of convolutional and pooling layers. In the convolutional layer, the activation (or feature) map from the previous layer is convolved using convolutional filter (or kernel) which is added with a bias and subsequently fed to the activation function to generate an activation map for the next layer. Meanwhile, the pooling layer (or subsampling layer) causes the activation maps to be reduced but, increases the invariance to distortion in the inputs. The convolutional and pooling layers are positioned to accomplish high level feature extraction. Also, a simple classifier, such as softmax, can be used in the last part of the CNNs.

Let $x_i^0 = (x_1, x_2..., x_n)$ be the data input vector, where n is the total number of samples in the ECG segment [48]. Next, the convolutional layer output is computed as follows

$$c_i^{l,k} = \sigma \left(b_k + \sum_{n=1}^{N} w_n^k x_{i+n-1}^{0k} \right) \qquad (1)$$

where l is the layer index, σ is the activation function producing nonlinearity, b is the bias for the kth activation map, N is the size of the filter, w_n^k is the weight for the nth filter index and kth activation map. Also, max pooling can be used to compute the maximum value in an input. The activation map in a layer is the pool using the following computation,

$$P_i^{l,k} = \max_{t \in T} (c_{iXS+r}^{l,k}) \qquad (2)$$

Where T is the window size of the pooling and S is the pooling stride. Thus, the activation map from layer to layer forward propagation is computed using the Eqs. (1) and (2). This includes initializing the weights and calculating the error cost minimization by using stochastic gradient descent on the ECG beats. After obtaining the predicted output, the loss function is used to calculate the prediction error. Then, back propagation is implemented to adjust the weights and the eror is predicted by calculating the slope of the convolutional weights. The process of forward and back propagation is continuously executed till the required number of epochs or other stopping criteria is met [48].

2.5. Structure

In this study, two 1-dimensional (1D) CNNs structures (Net 1 and Net 2) comprising of *four* convolutional layers, *four* max pooling layers and *three* fully connected layers are proposed. The pooling layer comes directly after the convolutional layer. Also, the striding of the filter over the input is set at 1 and 2 for convolutional and max pooling layers respectively. For Net 1 (2 s duration), the kernel size for all the max pooling layers are set at 2. In contrast, the kernel size for the alternating convolutional layers starting from layer 1 are set at 27, 15, 4 and 3 respectively. For Net 2 (5 s duration), the kernel size for all the max pooling layers are set at 2. The kernel size for the alternating convolutional layers starting from layer 1 are set at 26, 15, 3 and 4 respectively. Lastly, the neurons in layer 8 for both Net 1 and Net 2 are completely connected to 30, 10 and 2 neurons of layer 9, 10 and 11 respectively. For layer 1, 3, 5, 7, 9 and 10, leaky rectifier linear unit (LeakyRelu) [23] is implemented as an activation function and Xavier initialization [21] for the weights. Also, softmax function is used as a classifier in the last layer. The proposed structures of CNN (Net 1 and Net 2) is illustrated in Figs. 4 and 5 respectively. The structural details of the *two* networks are provided in Tables 3 and 4.

2.6. Training

For stochastic learning, back propagation [13] with batch size of 10 samples is employed. Accordingly, the weights are updated
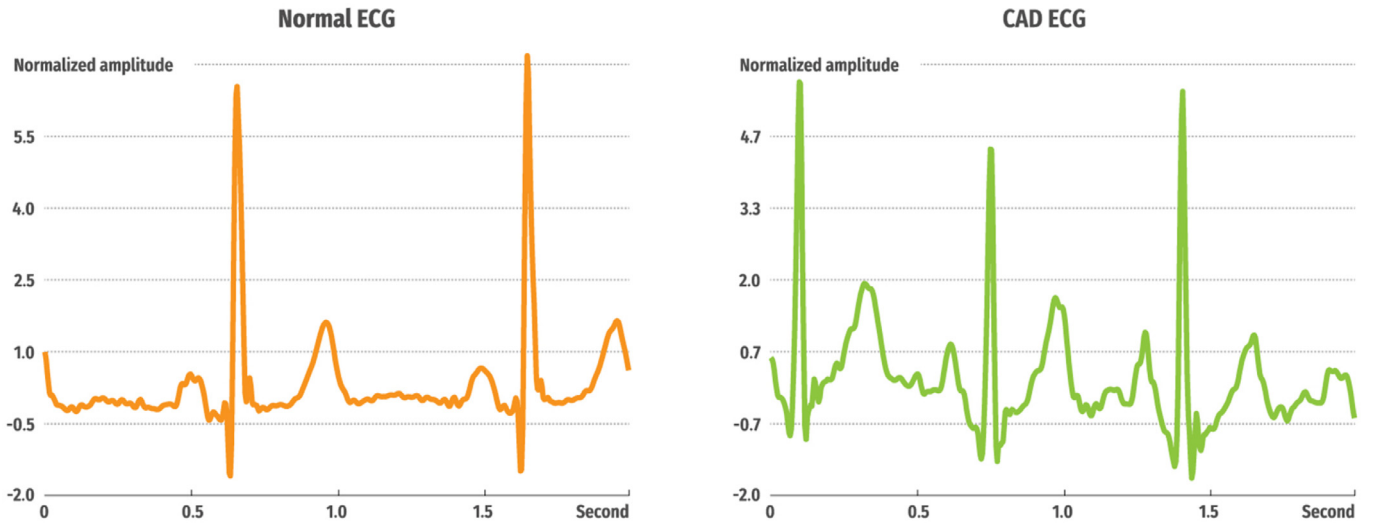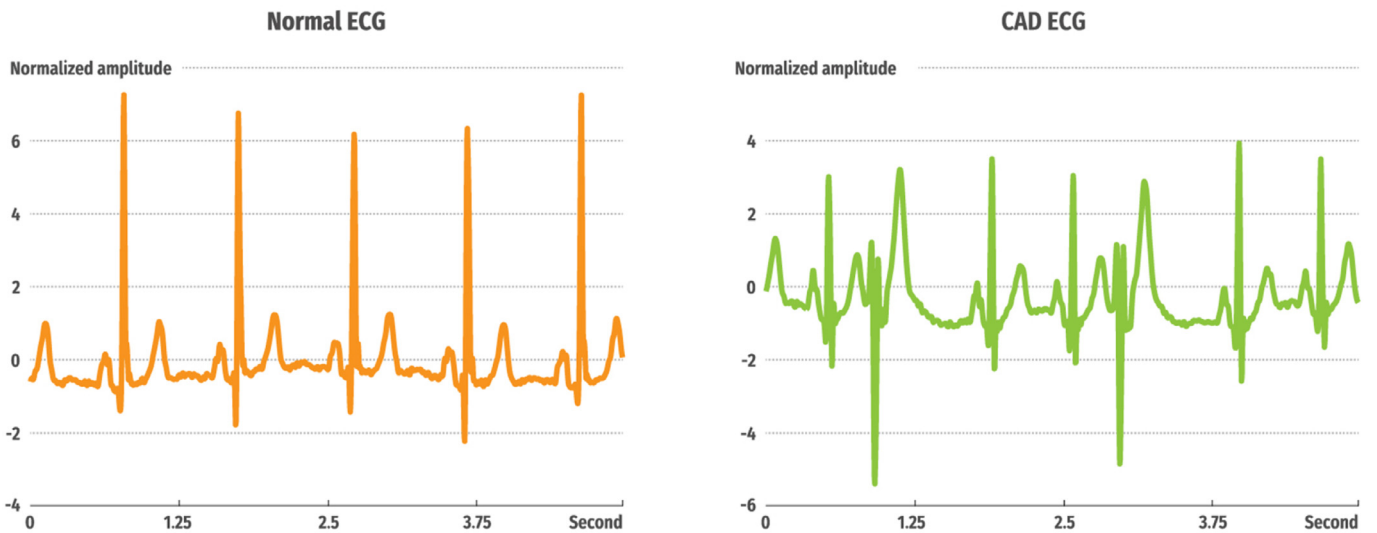
Fig. 2. Typical sketch of 2 s ECG signals (Net 1).

Fig. 3. Typical sketch of 5 s ECG signals (Net 2).

Table 3
The detailed overview of Net 1 structure.

Layers	Type	No. of neurons (output layer)	Kernel size for each output feature map	Stride
0–1	Convolution	488×5	27	1
1–2	Max-pooling	244×5	2	2
2–3	Convolution	230×10	15	1
3–4	Max-pooling	115×10	2	2
4–5	Convolution	112×10	4	1
5–6	Max-pooling	56×10	2	2
6–7	Convolution	54×10	3	1
7–8	Max-pooling	27×10	2	2
8–9	Fully-connected	30	–	–
9–10	Fully-connected	10	–	–
10–11	Fully-connected	2	–	–

using the following Eq. (3),

$$w_l = \left(1 - \frac{m_\lambda}{s}\right) w_{l-1}. - . \frac{m}{x} \frac{\partial c}{\partial w} \qquad (3)$$

where w is the weight, l is the layer number, m is the learning rate, λ is the regularization parameter, s is the total training samples, x is the batch size and c is the cost function. Also, the biases are

updated according to Eq. (4),

$$b_l = b_{l-1}. - . \frac{m}{x} \frac{\partial c}{\partial w} \qquad (4)$$

For this study, parameters such as regularization, learning rate and momentum are used to train the CNN structure. These parameters are set at 0.2, 0.003 and 0.7 respectively.
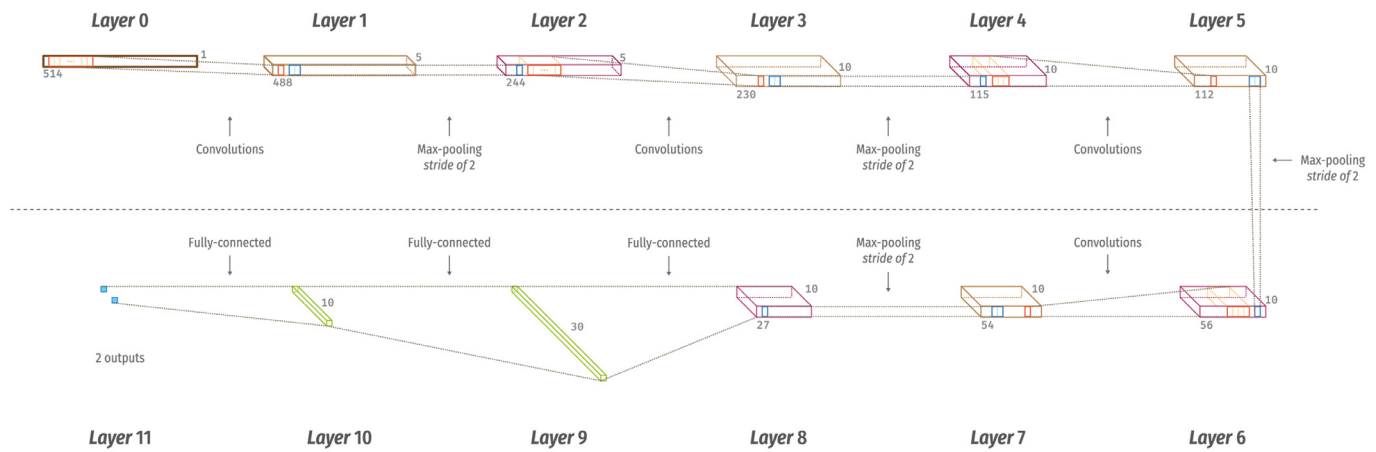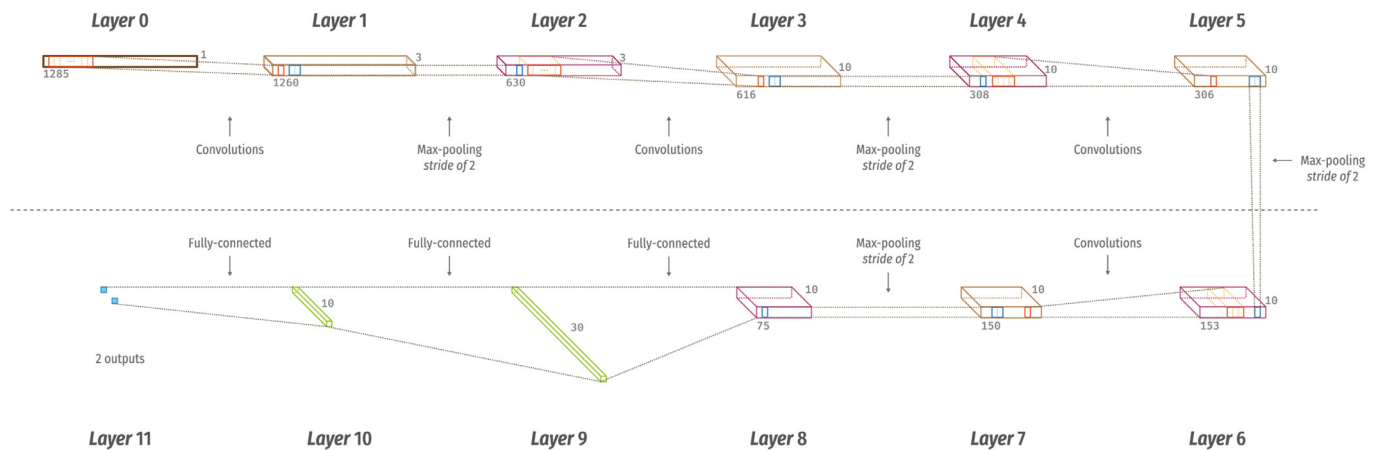
Fig. 4. The proposed CNN structure of Net 1.

Fig. 5. The proposed CNN structure of Net 2.

Table 4
The detailed overview of Net A structure.

Layers	Type	No. of neurons (output layer)	Kernel size for each output feature map	Stride
0–1	Convolution	1260×3	26	1
1–2	Max-pooling	630×3	2	2
2–3	Convolution	616×10	15	1
3–4	Max-pooling	308×10	2	2
4–5	Convolution	306×10	3	1
5–6	Max-pooling	153×10	2	2
6–7	Convolution	150×10	4	1
7–8	Max-pooling	75×10	2	2
8–9	Fully-connected	30	–	–
9–10	Fully-connected	10	–	–
10–11	Fully-connected	2	–	–

2.7. Testing

For every completed round of training epoch, the CNN model undergoes computational testing whereby 30% of the total training set (90%) are used for validation. In total, twenty epochs are iteratively run for both training and testing procedures. The distribution of ECG segments used for training and testing is illustrated in Fig. 6.

2.8. k-fold cross validation

The ten-fold cross validation technique [17] is implemented on both Net 1 (95,300 ECG segments) and Net 2 (38,102 ECG segments) by splitting the data in to *ten* parts. Of these, *nine* parts

are used to train and the remaining ECG segments are for testing. The process is iterated *ten* times by shifting the testing part. Simultaneously, classification performance (accuracy, specificity and sensitivity) is computed for every fold and the overall performance is obtained by taking the average of the *ten* folds.

3. Results

The experiment is conducted on a workstation with two Intel Xeon 2.40 GHz (E5620) processor and 24 GB RAM specification. Net 1 and Net 2 availed 3472.842 s and 1649.483 s respectively to complete an epoch.

The confusion matrix of the results for Net 1 is presented in Table 5. It can be noted from the table that, sensitivity of 95.18%
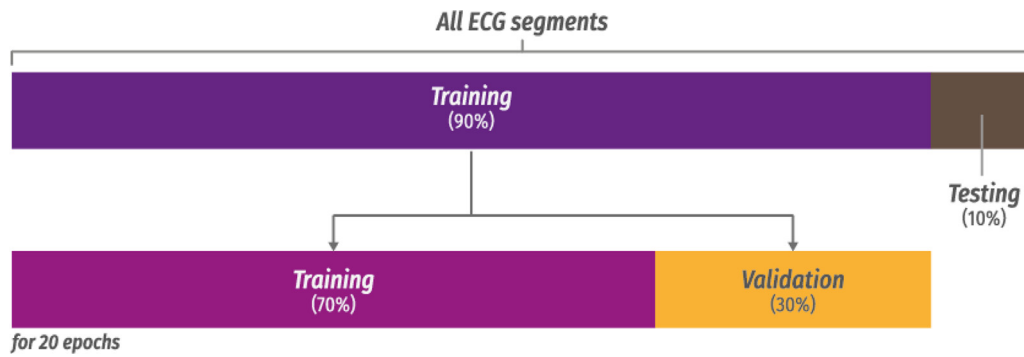
Fig. 6. An illustration of ECG segment distributions for training and testing sets.

Table 5
Confusion matrix for Net 1.

Original/ Predicted	Normal	CAD	Acc (%)	PPV (%)	Sen (%)	Spec (%)
Normal	76,146	3854	94.95	98.75	95.18	93.72
CAD	961	14,339	94.95	78.82	93.72	95.18

*Acc = accuracy, PPV = positive predictive value, Sen = sensitivity, Spec = specificity.

Table 6
Net 2 confusion matrix obtained using 10-fold cross validation.

Original/Predicted	Normal	CAD	Acc (%)	PPV (%)	Sen (%)	Spec (%)
Normal	30,680	1320	95.11	98.26	95.88	91.13
CAD	543	5577	95.11	80.86	91.13	95.88

*Acc = accuracy, PPV = positive predictive value, Sen = sensitivity, Spec = specificity.

Table 7
The overall classification performance for Net 1 (2 s) and Net 2 (5 s).

Segment length	TP	TN	FP	FN	Acc (%)	PPV (%)	Sen (%)	Spec (%)
2 s	14,339	76,146	3854	961	94.95	78.82	93.72	95.18
5 s	5577	30,680	1320	543	95.11	80.86	91.13	95.88

*TP = true positive, TN = true negative, FP = false positive, FN = false negative.
Acc = accuracy, PPV = positive predictive value, Sen = sensitivity, Spec = specificity

and specificity of 93.72% is obtained for the input of 2 s of ECG segment. In this work, 6.28% of the CAD ECG segments are wrongly identified as normal.

Table 6 shows the results obtained using 5 s of ECG duration. It can be noted from the table that, sensitivity of 95.88% and specificity of 91.13% is obtained. Also, out of the 6120 CAD ECG segments, 8.87% are incorrectly identified as normal.

Lastly, the overall classification performance for Net 1 and Net 2 is shown in Table 7. For Net 1, 94.95% accuracy, 93.72% sensitivity and 95.18% specificity is yielded. On the other hand, Net 2 achieved an accuracy of 95.11%, sensitivity of 91.13%, and specificity of 95.88%.

4. Discussion

The proposed deep learning structures (Net 1 and Net 2) for ECG signal characterization is motivated by its application to image analysis and classification [25,29]. Several studies have initiated the implementation of CNN for the automated characterization of abnormal ECG signals. Kiranyaz et al. [28] developed a patient specific ECG monitoring and categorizing system using *three* layer CNN structure. Their system used only R wave and detected ventricular and supraventricular ectopic beats with 99.00% and 97.60% accuracies respectively. Zubair et al. [48] trained a *three* layer CNN structure using derived R peak ECG beat patterns and yielded 92.7% ac-

curacy in detecting the *five* ECG classes. Acharya et al. [2] developed an *eleven* layer CNN structure to characterize the *four* ECG classes using *two* and *five* seconds of ECG signals. They reported 92.50% accuracy, 98.09% sensitivity and 93.13% for the *two* seconds of ECG signals. Also, their system obtained 94.90% accuracy, 99.13% sensitivity and 81.44% specificity for *five* seconds of ECG signals. In this study, alternative convolution and pooling layers are employed to derive robust deep features from the segmented ECG signals. Next, the features are linked to the fully connected layers for the ECG signal characterization. Our system negates the need for feature extraction, pre-processing, and classification stages. Thus, making the proposed system is suitable for real time monitoring of cardiac abnormalities.

Based on the results yielded in Tables 5–7, it can be argued that the algorithm implemented is significantly robust, reliable and efficient in deriving deep features and characterizing the input ECG signal. Moreover, the extraction and selection of the features and classification are combined into a single structure. Evidently, the performance of the CNNs structure have been validated with Net 1 and Net 2. The classification performance results of Net 1 (2 s) and Net 2 (5 s) are comparably superior as shown in Table 1.

In addition, the class of artificial neural networks formed by CNNs have shifting and scaling invariance properties. The model relies on the learn convolution kernels to reliably represent the

data. Thus, R peak detection is not performed as the segmented ECG signals are not affected by time scaling or shifting. The R peak detection is implemented in most of the works listed in Table 1.

The computational cost of the proposed system for the ECG signals characterization is relatively low. The algorithm is implemented in a computer with specifications of two Intel Xeon 2.40 GHz (E5620) processor and 24 GB RAM. Moreover, the proposed system only needs 1-Dimensional convolutions (multiplications and additions), hence implementation is economical and requires simple hardware. Therefore, the trained dedicated CNN can be used to characterize patient's long ECG signals efficiently and accurately. Also, Net 1 and Net 2 require 3472.842 s and 1649.483 s to complete an epoch.

The main advantages of our proposed system are summarized below:

1. The proposed CNNs structure is robust to shifting and scaling invariance.
2. QRS detection is not required.
3. Feature extraction, selection and classification procedures are combined in a single CNN structure.
4. Ten-fold cross validation ensures that, the results are reliable and robust.
5. The proposed system does not require extensive computational machinery. Thus, it is considerably easy to operate and cost effective.

The drawbacks of our proposed system are as follows:

1. The CNN requires lot of time (few hours) to train.
2. The training process requires huge database.
3. The length of the ECG signals for training and testing must be fixed, which depends on the structure of the CNN.

5. Conclusion

The CAD is the leading cause of heart attack. Therefore, a reliable and efficient automated diagnosis system is needed for an early detection of CAD. In this study, CNNs structures (Net 1 and Net 2) comprising of *four* convolutional layers, *four* max pooling layers and *three* fully connected layers are developed to detect *two* classes (normal and CAD). In total, 95,300 ECG segments of Net 1 (2 s) and 38,120 ECG segments of Net 2 (5 s) are used. The proposed system yielded 94.95% accuracy, 93.72% sensitivity and 95.18% specificity for Net 1 and 95.11% accuracy, 91.13% sensitivity and 95.88% specificity for Net 2. Our developed system can assist the clinicians to accurately diagnose CAD. Our method is simple to use, affordable and can be used for cardiac screening in developing nations. In future work, authors will be exploring possibility of improving the CNN structure with huge database. Also, this work can be extended for the early diagnosis of CAD, different stages of myocardial infarction (MI) and congestive heart failure (CHF) using ECG signals. This will help the clinicians to provide proper medication and save life.

References

[1] U.R. Acharya, H. Fujita, M. Adam, O.S. Lih, V.K. Sudarshan, T.J. Hong, J.E.W. Koh, Y. Hagiwara, C.K. Chua, C.K. Poo, T.R. San, Automated characterization and classification of coronary artery disease and myocardial infarction by decomposition of ECG signals: a comparative study, Inf. Sci. 377 (2017) 17–29.

[2] U.R. Acharya, H. Fujita, O.S. Lih, Y. Hagiwara, J.H. Tan, M. Adam, Automated detection of arrhythmias using different intervals of tachycardia ECG segments with convolutional neural network, Inf. Sci. 405 (2017) 81–90.

[3] U.R. Acharya, N. Kannathal, L.M. Hua, L.M. Yi, Study of heart rate variability signals at sitting and lying postures, J. Bodywork Mov. Ther. 9 (2005) 134–141.

[4] U.R. Acharya, O. Faust, V. Sree, G. Swapna, R.J. Martis, N.A. Kadri, J.S. Suri, Linear and nonlinear analysis of normal and CAD-affected heart rate signals, Comput. Methods Programs Biomed. 113 (1) (2014) 55–68.

[5] U.R. Acharya, V.K. Sudarshan, J.E.W. Koh, R.J. Martis, J.H. Tan, S.L. Oh, A. Muhammad, Y. Hagiwara, M.R.K. Mookiah, K.P. Chua, C.K. Chua, R.S. Tan, Application of higher-order spectra for the characterization of coronary artery disease using electrocardiogram signals, Biomed. Signal Process. Control 31 (2017) 31–34.

[6] American Heart Association, AHA., Heart disease and stroke statistics – 2016 update, 2016, A Report from the American Heart Association (AHA). Circulation, pp. e2–211.

[7] S. Arafat, M. Dohrmann, M. Skubic, Classification of Coronary Artery Disease Stress ECGs using Uncertainty Modeling, IEEE, 2005 1-4244-0020-1.

[8] S. Arafat, M. Dohrmann, M. Skubic, Classification of Coronary Artery Disease Stress ECGs using Uncertainty Modeling, IEEE, 2005 1-4244-0020-1.

[9] I. Babaoglu, O. Findik, M. Bayrak, Effects of principle component analysis on assessment of coronary artery diseases using support vector machine, Elsevier, Expert Syst. Appl. 37 (2010) 2182–2185.

[10] I. Babaoglu, O. Findik, E. Ulker, A comparison of feature selection models utilizing binary particle swarm optimization and genetic algorithm in determining coronary artery disease using support vector machine, Elsevier, Expert Syst. Appl. 37 (2010) 3177–3183.

[11] S.K. Bhatia, Chapter 2: coronary artery disease, in: Biomaterials for Clinical Applications, Springer, 2010, pp. 23–49.

[12] B. De, E.T. Cafiero, E. Jane-Llopis, et al., The Global Economic Burden of Non-communicable Diseases, Switzerland: World Economic Forum, Geneva, 2013.

[13] Bouvrie J. Notes on convolutional neural network, 2007.

[14] L.M. Buja, H.A. McAllister Jr, Coronary artery disease: pathological anatomy and pathogenesis, in: J.T. Willerson, J.N. Cohn, H.J.J. Wellens, D.R. Holmes (Eds.), Cardiovascular Medicine, 3rd ed., Springer, London, 2007, pp. 593–610.

[15] L.M. Buja, J.T. Willerson, The role of coronary artery lesions in ischemic heart disease: insights from recent clinicopathologic, coronary arteriographic, and experimental studies, Hum Pathol. 18 (1987) 451–461.

[16] M. Kumar, R.B. Pachori, U.R. Acharya, An efficient automated technique for CAD diagnosis using flexible analytic wavelet transform and entropy features extracted from HRV signals, Expert Systems with Applications 63 (2016) 165–172.

[17] R.O. Duda, P.E. Hart, D.G. Stork, Pattern Classification, 2nd ed., John Wiley and Sons, New York, 2001.

[18] J.P. Eckmann, D. Rueller, Ergodic theory of chaos and strange attractors, Rev. Mod. Phys. 57 (3) (1985) 617–656 part 1.

[19] O. Faust, R. Acharya, U.S. Krishnan, L. Min, Analysis of cardiac signals using spatial filling index and time-frequency domain, Biomed. Eng. Online 3 (1) (2004) 1–30.

[20] D. Giri, U.R. Acharya, R.J. Martis, S.V. Sree, T.C. Lim, T.V.I. Ahamed, J.S. Suri, Automated diagnosis of coronary artery disease affected patients using LDA, PCA, ICA and discrete wavelet transform, Knowl.-Based syst. 37 (2013) 274–282.

[21] X. Glorot, Y. Bengio, Understanding the difficulty of training deep feedforward neural networks, Aistats (2010).

[22] A.L. Goldberger, L.A.N. Amaral, L. Glass, J.M. Hausdorff, I. PCh, R.G. Mark, J.E. Mietus, G.B. Moody, C.-K. Peng, H.E. Stanley, PhysioBank, PhysioToolkit, and PhysioNet: components of a new research resource for complex physiologic signals, Circulation 101 (23) (2000) e215–e220.

[23] He K., Zhang X., Ren S., Sun J. Developing deep into rectifiers: surpassing human-level performance on image net classification, 1026–1034, 2015.

[24] R. Hoekema et al., Geometrical aspects of the interindividual variability of multilead ECG recordings, IEEE Trans. Biomed. Eng. 48 (5) (2001) 551–559.

[25] A.G. Howard, Some improvements on deep convolutional neural network based image classification, In: arXiv 1312 (2013) 5402.

[26] A. Kaveh, W. Chung, Automated classification of coronary atherosclerosis using single lead ECG, IEEE Conference Wireless Sensors, Kuching, Sarawak, 2013.

[27] W.S. Kim, S.H. Jin, Y.K. Park, H.M. Choi, A study on development pf multi-parameter measure of heart rate variability diagnosing cardiovascular disease, IFMBE Proc. 14 (2007) 3480–3483.

[28] S. Kiranyaz, T. Ince, M. Gabbouj, Real time patient specific ECG classification by 1-D convolutional neural network, IEEE Trans. Biomed. Eng. 63 (3) (2016) 664–675.

[29] A. Krizhevsky, I. Sutskever, G.E. Hinton, Imagenet classification with deep convolutional neural networks, in: Advances in Neural Information Processing systems, 2012, pp. 1097–1105.

[30] M. Kumar, R.B. Pachori, U.R. Acharya, Characterization of coronary artery disease using flexible analytic wavelet transform applied on ECG signals, Biomed. Signal Process. Control 31 (2017) 301–308.

[31] H.G. Lee, K.Y. Noh, K.H. Ryu, A data mining approach for coronary heart disease prediction using HRV features and carotid arterial wall thickness, IEEE, International Conference on Biomedical Engineering and Informatics, 2008.

[32] H.G. Lee, K.Y. Noh, K.H. Ryu, in: Mining Biosignal data: Coronary Artery Disease Diagnosis using Linear and Nonlinear Features of HRV, Springer-Verlag Berlin Heidelberg, 2007, pp. 218–228.

[33] S.C. Lee, Using translation-invariant neural network to diagnose heart arrhythmia, in: Proceedings of IEEE Conference Neural Information Processing Systems, 1989, pp. 2025–2026.

[34] R. Lehtinen, H. Holst, V. Turjanmaa, L. Edenbrandt, O. Pahlm, J. Malmivuo, Artificial neural network for exercise electrocardiographic detection of coronary artery disease, 2nd International Conference on Bioelectromagnetism, Melbourne Australia, February, 1998.

[35] K. Lewenstein, Radial basis function neural network approach for the diagnosis of coronary artery disease based on the standard electrocardiogram exercise test, Med. Biological Eng. Comput. 39 (2001) 1–6.

[36] C.D. Mathers, D. Loncar, Projections of global mortality and burden of disease, PloS Med 3 (11) (2006) 2002–2030 e422, doi:10.1371/journal.pmed.0030442.

[37] S. Mendis, et al., Global Status Report on Non-Communicable Diseases, 2014 World Health Organization, 2014.

[38] S. Patidar, R.B. Pachori, U.R. Acharya, Automated diagnosis of coronary artery disease using Tunable-Q wavelet transform applied on heart rate signals, Knowl.-Based Syst. 82 (2015) 1–10.

[39] D.M. Schreck, L. Ng, B.S. Schreck, S.F. Bosco, J.R. Allegra, D. Zacharias, J.V. Wortzel, Detection of coronary artery disease from the normal resting ECG using nonlinear mathematical transformation, Annals Emerg. Med. 17 (1988) 132–134.

[40] B.N. Singh, A. Tiwari, Optimal selection of wavelet basis function applied to ECG signal denoising, Digit. Signal Process. 16 (3) (2006) 275–287.

[41] S. Sood, M. Kumar, R.M. Pachori, U.R. Acharya, Application of empirical mode decomposition-based features for analysis of normal and CAD heart rate signals, J. Mech. Med. Biol. 16 (1) (2016).

[42] J.E. Tarride, M. Lim, M. DesMeules, et al., A review of the cost of cardiovascular disease, Can J Cardiol. 25 (2009) e195–e202.

[43] N. Townsend, K. Wickramasinghe, P. Bhatnagar, K. Smolina, M. Nicholas, J. Leal, R. Luengo-Fernandez, M. Rayner, Coronary Heart Disease statistics, a Compendium of Health Statistics, British Heart Foundation, London, 2012 ed.

[44] N. Townsend, J. Williams, P. Bhatnagar, K. Wickramasinghe, M. Rayner, Cardiovascular Disease Statistics, British Heart Foundation, London, 2014.

[45] J.T. Willer, L.D. Hillis, L.M. Buja, Ischemic Heart Disease Clinical and Pathophysiological Aspects, New York, Raven, 1982.

[46] W.H. Organization, in: Global Health Estimates: Deaths by Cause, Age, Sex and Country, WHO, Geneva, 2014, pp. 2000–2012.

[47] L. Yin, Y. Chen, W. Ji, A novel method of diagnosing coronary heart disease by analyzing ECG signals combined with motion activity, IEEE International workshop on machine learning for signal processing, China, Beijing, 2011 September 18-21.

[48] M. Zubair, J. Kim, C. Yoon, An automated ECG beat classification system using convolutional neural networks, in: 6th International Conference on IT Convergence and Security (ICITCS), 2016, pp. 1–5.